The Separation of Light Gaseous Isotopes by Mass Diffusion Columns II

By W. J. DE WET * and J. LOS

FOM-Laboratorium voor Massascheiding, Kruislaan 407, Amsterdam-O, Netherlands

(Z. Naturforschg. **19 a**, 747—755 [1964]; eingegangen am 31. Oktober 1963)

The design of mass diffusion columns operated with partition membranes, for the separation of light gaseous isotopes, is discussed. A theoretical analysis of experimental results obtained indicates that a good agreement between experimental results and theory is only obtained at low column pressures and moderate countercurrent flow rates. At fairly low countercurrent flow rates mixing effects due to viscous dragging and gas solubility by the condensate appear to be considerable whereas excessively high countercurrent flow rates, on the other hand, also seem undesirable. Some suggestions are proposed to obviate impairing effects at least to some extent.

The preceding paper [1] (Part I) dealt with a theoretical treatment of mass diffusion columns with particular emphasis on columns in which the countercurrent is facilitated by utilising a thin partition membrane of low permeability. This paper continues with a description of two laboratory columns, both containing membranes and designed according to principles developed in Part I. Experimental work, including a comparison of theory with experimental results, is then described.

The same notation of symbols introduced in Part I, is used in this paper.

3. Design of Columns

According to the theoretical investigation it is necessary to design columns in such a way that the membrane divides the gas present in the column in approximately equal quantities. It is furthermore important that only a small fraction of the gas in the column diffuses into the vapour supply tube. The simplest way to evaluate suitable values for the membrane and vapour supply tube radii and for the vapour consumption rate to comply with these restrictions, is to consider the column to be of plane design. This assumption is permissible for all practical cases provided the eventual value of r_1/r_2 for the column is larger than 0.5.

The equivalent of equation (10) for the plane case may analogously be derived from equation (7), and is given by

$$\gamma = \gamma_2 \exp\{-u\,x/n\,D_{01}\} \qquad (38)$$

for $\varepsilon \ll 1$ (or $N \approx 1$), where x is the coordinate perpendicular to the condenser, with its origin on the condenser surface, as shown in Fig. 4. Since u remains constant under stationary conditions, equation (38) may be applied to the three distinct regions graphically depicted in Fig. 4, as follows

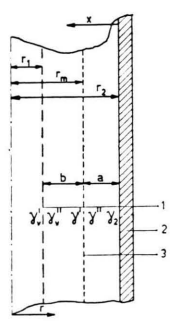

Fig. 4. Details concerning the design of mass diffusion columns operated with partition membranes. 1. vapour supply tube wall. 2. condenser. 3. partition membrane.

$$\begin{aligned} \gamma &= \gamma_2\, e^{-\Theta x} && (0 \leqq x \leqq a), \\ \gamma &= \gamma'\, e^{-\Theta(x-a)} && (a \leqq x \leqq a+b), \\ \gamma &= \gamma_v'\, e^{-\Theta(x-a-b)} && (a+b \leqq x < \infty) \end{aligned} \qquad (39)$$

where Θ is $u/n\,D_{01}$ and γ', γ'', γ_v' and γ_v'' (introduced below) are the mole fractions of gas on the sides of the partition membrane and the vapour supply tube, respectively. The distances a and b represent the width between the condenser and the membrane and the width between the membrane and the vapour supply respectively.

Direct application of the latter equations yields

$$\gamma'' = \gamma_2\, e^{-\Theta a} = \gamma'\, e^{\Theta\, d/\lambda}, \qquad (40)$$

$$\gamma_v'' = \gamma'\, e^{-\Theta b} = \gamma_v' \exp\{\Theta\,(d/\lambda)_v\}, \qquad (41)$$

where $(d/\lambda)_v$ is the diffusion resistance of the wall

* On attachment from the South-African Atomic Energy Board, Pelindaba, Pretoria.

[1] W. J. DE WET and J. LOS, Z. Naturforschg. **19 a**, 740 [1964].

of the vapour supply tube. In this ratio, analogously as for the partition membrane, d represents the wall thickness and λ the fraction of the surface area available to flow for the vapour supply tube.

Substituting

$$r_2 - r_m = a \quad \text{and} \quad r_m - r_1 = b$$

equations (40) and (41) yield

$$\exp\{-(r_2 - r_1)\,\Theta\} = \frac{\gamma_v'}{\gamma_2} \exp\{\Theta[d/\lambda + (d/\lambda)_v]\}\,. \tag{42}$$

Equation (42) clearly indicates the dependence of the appropriate value of $(r_2 - r_1)$ on the vapour consumption, the total diffusion resistance $[d/\lambda + (d/\lambda)_v]$ and the ratio γ_v'/γ_2, which is a function of the fraction of gas present in the vapour supply tube. For equal partition of the gas in the column by the membrane

$$\int_0^a \gamma\, dx = \int_a^{a+b} \gamma\, dx \tag{43}$$

assuming $\gamma_v'/\gamma_2 \cong 0$. Equation (43) reduces to

$$[1 - \exp\{\Theta(r_2 - r_m)\}]\, e^{\Theta\, d/\lambda} = [\exp\{-\Theta(r_m - r_1)\} - 1]\,. \tag{44}$$

By specifying the ratio γ_v'/γ_2 it is thus possible to evaluate $(r_2 - r_1)$ from equation (42) for a given system. From this result the values of $(r_2 - r_m)$ and $(r_m - r_1)$ may be easily obtained from equation (44).

When designing a column two approaches are consequently possible, namely, if fixed values for r_1 and r_2 are chosen and the values of d/λ and $(d/\lambda)_v$ are known, appropriate values for r_m and u (or Θ) can be evaluated, or, for given d/λ and $(d/\lambda)_v$ values r_1 and r_m can analogously be calculated for given r_2 and Θ values. Due to practical considerations the first procedure was followed by us.

The columns used in this investigation are shown in Figs. 5 and 6. They will subsequently be referred to as Column I and Column II respectively. Column I [2] was almost completely made from glass and was used for separation factor determinations at total reflux only. The radius r_2 was 2.25 cm and it possessed an effective column length of 80 cm. Column II, on the other hand, was made of stainless steel and was utilised for both

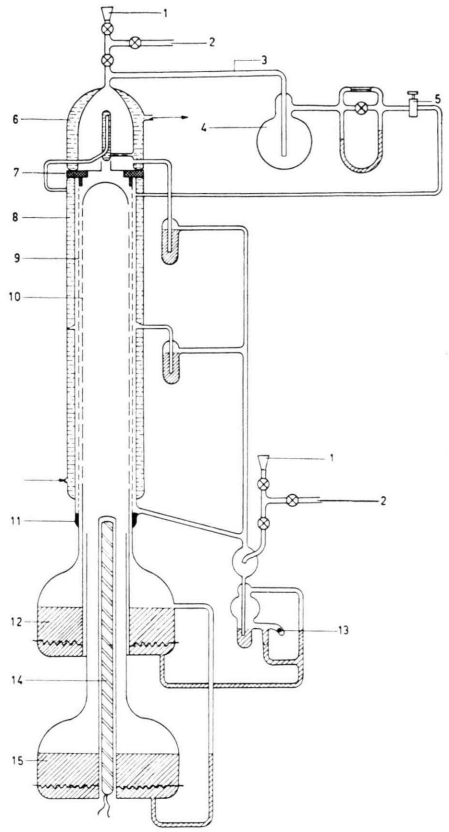

Fig. 5. Schematic diagram of Column I.

1. sample ports.
2. vacuum line.
3. countercurrent return tube.
4. buffer volume.
5. flow regulator.
6. top condenser.
7. metal flange (with O-ring seals).
8. condenser.
9. partition membrane.
10. vapour supply tube.
11. mercury seal.
12. auxiliary boiler (0.5 KW).
13. vapour consumption meter.
14. super heater (0.5 KW).
15. main boiler (1.5 KW).

separation factor as well as separative power determinations. The radius of this column was 4.5 cm and its effective column length was 140 cm.

The partition membranes used in these columns were made of stainless steel gauze having 25,000 holes per cm^2. The average diameter of the holes was 8 μ and the membrane thickness was 0.01cm. The value of d/λ for these membranes was approximately 0.8 cm. Column I was supplied with a vapour supply tube containing 480 holes with an average radius of 1.1 mm. The holes were equally spaced in line around the circumference of the tube (16 holes per row with about 3 cm in between successive rows). This pattern of peri-

[2] This column was originally constructed by Ir. C. J. G. Slieker of this laboratory by following the details provided by Gverdtsiteli et al. [3]. For this investigation the column was modified in several respects.

[3] L. G. Gverdtsiteli, R. Y. Kucherov, and V. K. Tskhakaya, U.N. Peaceful Uses of Atomic Energy, 2nd Int. Conf., 1958.

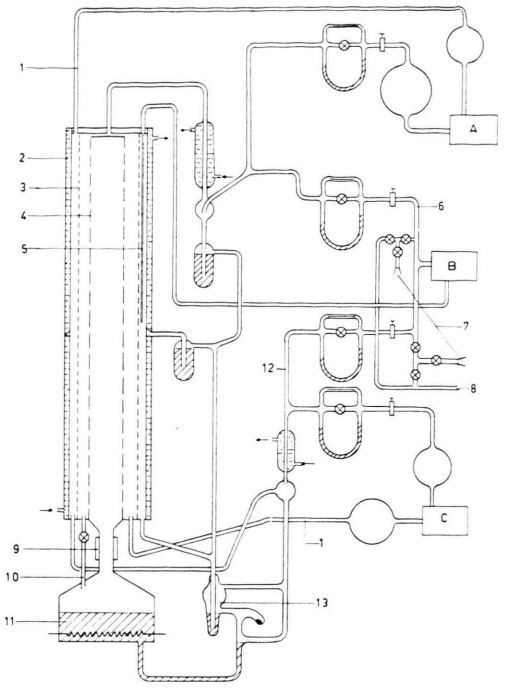

Fig. 6. Schematic diagram of Column II.
A, B and C are three gas circulating pumps.

1. countercurrent return tubes.
2. condenser.
3. partition membrane.
4. vapour supply tube.
5. feed tube (2 mm I. D.).
6. product line.
7. sample ports.
8. vacuum line.
9. super heater (0.5 KW).
10. vapour by-pass tube.
11. boiler (3.5 KW).
12. waste line.
13. vapour consumption meter.

odical arrangement of the holes was originally used by GVERDTSITELI et al.[3], who attached some additional physical significance to such an array. Te tube radius was 1.55 cm and its $(d/\lambda)_V$ value approximately 6.4 cm. Column II was, however, fitted with a metal vapour supply tube in which the holes were drilled evenly distributed over the whole exterior surface of the tube. It contained one hole per cm² with a diameter of 1.3 mm. The tube radius was 2.5 cm and its $(d/\lambda)_V$ was about 12.4 cm. Using these data and accepting a tolerance of 0.1% for the ratio γ_V'/γ_2, the appropriate values of Θ, according to equation (42), are 0.88 and 0.454 cm^{-1} for the two columns respectively. For the separation of Ne isotopes, using water as working liquid, the u values are $1.63 \cdot 10^{-5}$ and $8.4 \cdot 10^{-6}$ mol/cm² sec, respectively. The value used for D_{01} is that given in Table I. The corresponding boiling rates required in the columns were 20 and 36 ml liquid/min. For the above vapour consumption rates the membrane positions were calculated from equation (44). The value of r_m eventually used for Column I, was slightly less (0.7 mm) than the calculated value, thus attempting to compensate for the thickness of the condensate film running down the condenser wall. The r_m values used were 2 and 3.9 cm respectively. The widths of the upward streams were consequently two to three times the widths of the downward streams. For theoretical purposes the r_2 value of Column I was subsequently taken as 2.2 cm.

It should be reminded that in the above treatment it was tacitly assumed that the flow of vapour through the partition membrane and the vapour supply wall takes place by a diffusion process only. In practice, however, small hydrodynamical pressure differences exist which obviously contribute to the flow of vapour through them. These combined phenomena presumably create larger gas pressure gradients across the partition membrane and vapour supply tube wall than that calculated assuming diffusional flow only, for the same vapour consumption. For limiting the fraction of gas diffusing back into the vapour supply tube this predicts a favourable effect. On the other hand, unfortunately, it means that a relatively larger fraction of the gas in the column is forced into the space between the partition membrane and the condenser. To eliminate this the membranes should be shifted closer to the condensers than the positions inferred by equation (44). This was, however, not accounted for in our columns.

4. Experimental Procedure

Although our columns were basically similar to those used by GVERDTSITELI et al.[3] they were operated quite differently. Instead of using a fixed flow resistance in the tube combining the upward and downward streams at the top of the column and controlling the amount of auxiliary vapour additionally entering the lower part of the column in the space between the membrane and the vapour supply tube, in order to regulate the magnitude of the countercurrent, we proceeded as follows.

By means of a flow regulator in the countercurrent flow return tube (see Figs. 5 and 6), the flow rate of the countercurrent stream could be conveniently regulated and adjusted. It was further observed experimentally that the amount of additional vapour entering the upward stream has no significant influence on the performance of a column provided its ratio to the total vapour consumption in the column remains small. In Column I the auxiliary boiler was simply set at a slow boiling rate and was kept the same throughout all the experiments. In Column II, the metal tap which served to control the fraction of auxiliary vapour by-passed to the upward stream, was set at a small opening which also remained unaltered during experiments. For a constant boiling rate of the main boiler, no measurable variation of the vapour consumption was observed in experiments in which the flow rate of the countercurrent stream was varied.

Due to the large surface area of the partition membrane and the relatively low vapour consumption rate used in Column II, the pressure drop across its membrane was not sufficient to enable the high countercurrent flow rates required in this column. Two gas circulation pumps were consequently used, which are shown in Fig. 6. This was not necessary for Column I.

The third pump shown in Fig. 6 served to pump the combined product and waste streams, as a new feed stream, back to the middle of the column. This method of drawing product and waste streams is very suitable for testing column performances and possesses the further advantages that no losses occur and that the total column pressure remains constant, which is only hardly feasible otherwise. All separative power determinations were done under symmetrical take-off conditions. With the arrangement of flowlines and flowmeters used in Column II the effect of the magnitude of the countercurrent on the variation of the separative power with the magnitude of the product stream, could be conveniently studied.

Although the columns were purposely designed for the separation of Ne isotopes, using water as working liquid, Column I was also tested with other liquids (m-xylene and 1,1 – 2,2-tetrachloroethane) for the same separation. Column II was not suitable for the use of liquids other than water but was tested for the separation of H_2 and D_2. Separation factors for H_2 and D_2 were also determined in Column I with water as working liquid only. The Ne isotopes used were of natural abundance and were obtained from a commercial cylinder. The $H_2 - D_2$ mixtures used in both columns were admixed from pure gases when filling the column. The D_2 contents of these mixtures were between 3 and 5%. No difficulties due to chemical exchange between H_2 and D_2 were encountered even after prolonged continuous use of the same mixture in the column.

The flow rates in the columns were measured with calibrated capillary flowmeters containing dibuthylphthalate. Small samples were drawn from the columns for the separation factor determinations. All the samples were mass spectrometrically analysed. The equilibrium times of the columns were only a few hours but samples were mostly taken after about 24 hours of steady operation.

5. Details Concerning the Theoretical Analysis of the Experimental Results and a Discussion of Possible Mixing Effects

In order to compare the experimental results obtained from Columns I and II with the theory it is necessary to acquire values for various diffusion coefficients. Since ε and D_{01}/D_{12} are almost independent of temperature and high accuracies are obviously not essential, diffusivities were calculated from the HIRSCHFELDER equation and other data reported by REID and SHERWOOD [4], by assuming average temperatures. Unfortunately, the force constants and collision integrals for Ne in 1,1 – 2,2-tetrachloroethane could not directly be calculated due to lack of data for this system. By using the data available for CCl_4, however, an approximate value was estimated. The values obtained (for a pressure of 1 atm) together with the analogously calculated ε values for the various systems, are given in Table I.

Isotopic Pair	Working Liquid	D_{01} cm^2 sec^{-1}	D_{12} cm^2 sec^{-1}	ε
Ne^{20}, Ne^{22}	H_2O	0.49	0.57	0.0205
Ne^{20}, Ne^{22}	$C_2H_2Cl_4$	0.13	0.54	0.0415
H_2, D_2	H_2O	1.07	1.42	0.258

Table I. Calculated D_{01}, D_{12} and ε values.

The only remaining unknown factor needed for a theoretical analysis of the experimental results, by utilising equations (32) to (37), is γ_2. This is also the only factor in these equations which is slightly pressure dependent since the product $n D_{01}$ is about constant. This implies that for theoretical considerations, column efficiencies may be considered as almost independent of the column pressure. Pressure corrections may nevertheless be introduced by substituting

$$\gamma_2 = (p - p_{vap})/p$$

where p is the column pressure and p_{vap} is the vapour pressure of the working liquid at the condenser temperature. In our experiments the temperature of the cooling water was about 20 °C for which the vapour pressures of water and 1,1 – 2,2-tetrachloroethane are approximately 20 and 5 mm Hg, respectively.

To conform to the symmetrical take-off conditions in the experiments with Column II the theoretically calculated values of the separative power obtained from equation (33) were reduced by 20% [5]. The broken lines in the subsequent figures give the theoretically expected results, pertaining to similar experimental conditions, for the various experiments.

Direct correlation of the experimental results with the theory is considerably obscured in that various impairing parasitic currents and flow mixing effects exist in mass diffusion columns which primarily depend on the experimental conditions [3]. Such currents and effects would cause mixing of isotopes of different concentration and may arise from convection streams (and gravitational flows due to composition variations in the radial direction) asym-

[4] R. C. REID and T. K. SHERWOOD, The Properties of Gases and Liquids, McGraw-Hill Book Co., Inc., New York 1958.

[5] J. Los, D. Sc.-thesis, University of Leyden, 1963.

metric or irregular flow patterns in the upward and downward streams, viscous dragging by the down flowing condensate and due to gas solubility of the isotopes in the condensate at the condenser. Effects due to the latter, however, should only be noticeable when the amount of gas dissolved and carried away by the condensate is an appreciable fraction compared to the total countercurrent flow. Consequently in columns in which the countercurrent flow rate is fairly small, the volume of condensate draining down the condenser is relatively large and the column pressure and isotope solubilities are also appreciable, adverse mixing due to this should be expected to be quite serious. As explained by GVERDTSITELI et al.[3] viscous dragging effects caused by the condensate film flowing down the condenser should not be significant as long as the circulation velocity in the downward stream exceeds the surface velocity of the condensate film. For small countercurrent flow rates and large condensate volumes, however, such mixing effects are surely considerable especially at high column pressures. Theoretically the optimum countercurrent flow is almost independent of the column pressure and hence the circluation velocity should decrease (the molar flow remains constant) for a given system when the column pressure is increased. Mixing effects due to gas capture by the liquid film will consequently become more serious if the column pressure is raised. The amount of gas dragged along also increases with pressure, which obviously further enhances this mixing effect. Asymmetric flow effects only seem important at excessively high countercurrent flow rates.

A radial temperature gradient and viscosity variation according to composition gradients could also influence the flow profile and this will inevitably always be inherently associated to real columns.

To facilitate the subsequent discussions Table II was compiled from various data applicable to the experimental conditions of our experiments.

The values of the percentage ratio given in Table II were calculated from solubility values determined by us. The BUNSEN absorption coefficients measured at 18 °C were for Ne, 0.0103 and 0.0296 in water and $C_2H_2Cl_4$ respectively, and for H_2, 0.0186 in water. The average surface velocities of the condensates were calculated from the following formula

$$u_{\text{aver.}} = \frac{\varrho\, g}{4\,\mu}\left(\frac{V\,\mu}{80\, r_2\, \varrho\, g}\right)^{2/3}$$

where

$u_{\text{aver.}}$ is the average surface velocity of the condensate film (cm/sec).
ϱ is the density of the condensate (g/cm³).
μ is the viscosity of the condensate (poise).
V is the draining rate of the condensate (cm³/min).
g is the gravitational constant (cm/sec²).

The viscosity of both water and $C_2H_2Cl_4$ at 20 °C is about $1 \cdot 10^{-2}$ poise.

6. Discussion of the Experimental Results

a) The separation factor determinations at total reflux

The effect of the magnitude of the countercurrent on the separation factor at total reflux has been

Experiment (refering to the figures)	γa	γb	L_0 (theor.) (mol/sec)	Draining rate of the condensate (cm³/min)	Average surface velocity of the condensate film (cm/sec)	Average velocity of the downward stream at L_0 (theoret.) (cm/sec)	Percentage ratio of the amount of gas dissolved and drained away by the condensate to the gas flow in the downward stream at L_0 (theoret.)
7 b	0.686	0.015	$1.58 \cdot 10^{-5}$	122	9.8	0.09	9.88
c						0.19	17.40
d						0.34	35.80
8 b	0.825	0.459	$3.05 \cdot 10^{-4}$	20	2.6	1.56	<0.1
c						5.96	<0.1
9 b	0.847	0.336	$5.16 \cdot 10^{-4}$	36	2.4	0.43	<0.1
c						0.91	<0.1
d						1.46	<0.1
10 b	0.912	0.592	$1.75 \cdot 10^{-3}$	36	2.4	1.25	<0.1
c						3.02	<0.1

Table II. Estimated approximate values of various magnitudes and ratios together with miscellaneous experimentally measured quantities applying to the various experiments.

studied in both columns for various systems and column pressures. The results obtained are given in Figs. 7, 8, 9 and 10. Although all these results are in agreement with the theory in that an optimum countercurrent flow rate exists for which a column attains a maximum separation factor, the various curves display apparently contradicting discrepancies from their respective theoretical curves.

In the first instance the results in Fig. 7 indicate that the experimentally measured optimum countercurrent flow rate is larger than the theoretically predicted value and still increases if the column pressure is increased. A similar phenomenon was found by GVERDTSITELI et al.[3] for the separation of Ne isotopes with xylene as working liquid, who ascribed this to viscous dragging caused by the down flowing condensate. Due to the large differences between the average surface velocity of the condensate film and the circulation velocities in the downward streams for the experiments in Fig. 7, as indicated by Table II, these results were most probably drastically affected. This also explains why the experimentally measured optimum countercurrent flow rates occur at comparatively high flow rates in this set of experiments. The isotope solubilities in these experiments are also considerable (see Table II) and effects due to this will have an analogous influence on the experimentally measured optimum countercurrent flow rate. It is furthermore reasonable to expect that for columns in which the countercurrent flow rate is small and draining rate of condensate is large, that the optimum countercurrent should further increase, due to increased viscous dragging as well as solubility effects, if the column pressure is increased and that the efficiency of the column is correspondingly adversely affected. This is confirmed by the results in Fig. 7. Asymmetric flow effects in these experiments are, however, not expected to be quite serious, which is possibly not the case in experiments when much higher countercurrent flow rates are used. Satisfactory agreement between the theory and the experimental results in Fig. 7 is consequently only expected at low column pressures and at relatively high countercurrent flow rates, which is indeed the case.

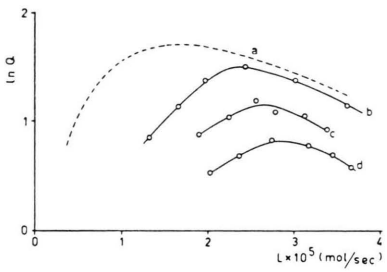

Fig. 7. The effect of the countercurrent flow rate on the separation factor at total reflux for Column I.
Separated mixture: Ne^{20}, Ne^{22}. Working liquid: $C_2H_2Cl_4$.
$u = 1.73 \cdot 10^{-5}$ mol/cm² sec.

Curve	a (calc.)	b (exp.)	c (exp.)	d (exp.)
p (mm Hg)	200	210	370	760

The results in Figs. 8 and 9 are also in fair agreement with the theory except that for Column II the separation factors deviate notably from the calculated values at the high countercurrent flow rates. Furthermore, the effect of the column pressure on the value of the optimum countercurrent flow rate shows just the opposite trend than the behaviour depicted by the results in Fig. 7. Since the theoretically and experimentally determined optimum countercurrent flow rates show satisfactory agreements, mixing effects due to viscous dragging and gas solubility by the condensate film seem relatively insignificant when comparing the conditions in Table II of these experiments with those of Fig. 7. A more reasonable explanation is supposedly that flow mixing effects at higher countercurrent flow rates become more mitigating on the separation at the higher column pressures. As in agreement with the experimental observations the effect of the column pressure on the column efficiencies in these experiments should be less pronounced than that depicted by the results in Fig. 7.

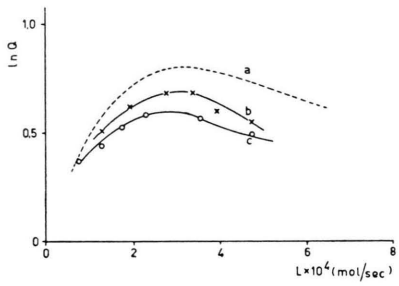

Fig. 8. The effect of the countercurrent flow rate on the separation factor at total reflux for Column I.
Separated mixture: Ne^{20}, Ne^{22}. Working liquid: H_2O.
$u = 1.63 \cdot 10^{-5}$ mol/cm² sec.

Curve	a (calc.)	b (exp.)	c (exp.)
p (mm Hg)	200	215	760

The rather drastic discrepancies of all the experimental curves in Fig. 9 from the theoretical curve at the right-hand side of the optimum enrichments seem to be associated with mixing effects due to the excessively high countercurrent flow rates, independent of the column pressure. To our opinion this cannot be attributed to any of the mixing effects considered in section 5, other than the flow mixing effects mentioned. Although even at these high flow rates steady laminar flow stability should prevail it might be possible that at either end of the column ineffective lengths exist in which a stable radial pressure gradient of the gas is not yet established. It is, however, almost impossible to make any estimate concerning the total value of such lengths and their dependence on the countercurrent flow rate.

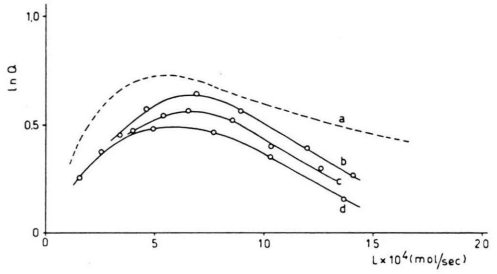

Fig. 9. The effect of the countercurrent flow rate on the separation at total reflux for Column II.
Separated mixture: Ne^{20}, Ne^{22}. Working liquid: H_2O.
$u = 8.4 \cdot 10^{-6}$ mol/cm² sec.

Curve	a (calc.)	b (exp.)	c (exp.)	d (exp.)
p (mm Hg)	200	200	360	760

For the separation of H_2 and D_2 in Column II even higher countercurrent flow rates were required than for separation of Ne isotopes and the results given in Fig. 10 appear to be similarly but more seriously affected. In these results, however, the separation factor does not improve considerably when lowering the column pressure and furthermore the experimentally optimum countercurrent flow rates are only about half the theoretical value. If the calculated ε value for this system is indeed of the right magnitude, the experimental results obtained are rather disappointing. To reduce the countercurrent flow rates required for the separation of H_2 and D_2 it is necessary to use an auxiliary vapour in which the diffusivities of these gases are much less than in water vapour. Higher efficiencies should then be achieved if the rather poor results in Fig. 10

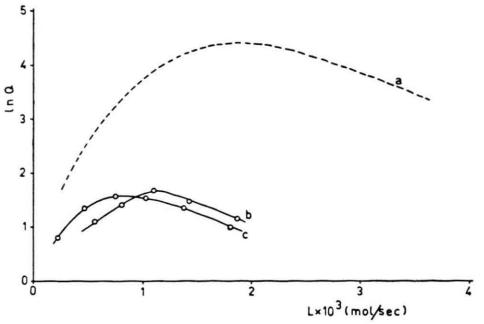

Fig. 10. The effect of the countercurrent flow rate on the separation factor at total reflux for Column II.
Separated mixture: H_2, D_2. Working liquid: H_2O.
$u = 8.4 \cdot 10^{-6}$ mol/cm² sec.

Curve	a (calc.)	b (exp.)	c (exp.)
p (mm Hg)	200	320	760

are solely a result of impairing effects caused by the high countercurrent flow rates. A maximum separation factor of 2.2 obtained for the same system in Column I, was even more disappointing. Apart from mixing or other undesirable effects a considerable amount of the gas in the column presumably diffuses into the vapour supply tube which was possibly further responsible for this low column efficiency.

Only a single experiment with m-xylene as working liquid in Column I was performed for the separation of Ne isotopes. At a column pressure of 175 mm Hg the separation factor obtained was 5.2 which is about the same as that obtained by GVERDTSITELI et al.[3] for the same system, if column length differences are corrected for.

b) The separative power determinations

In Figs. 11, 12 and 13 the results of the separative power determinations for the separation of Ne isotopes with water as working liquid in Column II, are given. These results are in excellent agreement with the theory in that it provides evidence that the maximum separative power obtainable from a column is a function of the magnitude of the countercurrent flow rate and should increase proportionally to the ratio $m^2/(1+m^2)$. The experimental curve in Fig. 13, however, approaches the limiting maximum separative power at somewhat lower m values than that predicted by the theoretical curve. For $m > 2$ the experimental maximum separative power is almost constant for all practical reasons, which is to be expected according to the above discussions.

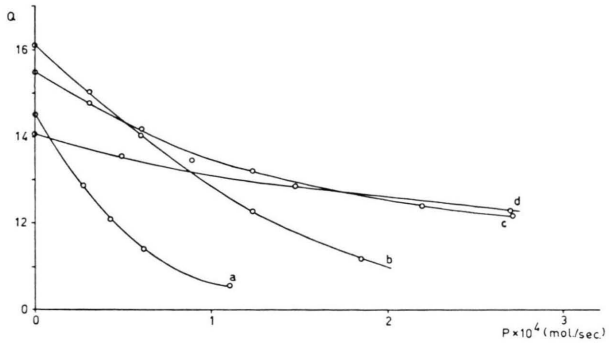

Fig. 11. The effect of the size of the product stream on the separation factor of Column II for various m values. Separated mixture: Ne^{20}, Ne^{22}. Working liquid: H_2O. $p=760$ mm Hg. $u=8.4\cdot10^{-6}$ mol/cm² sec.

Curve	a	b	c	d
$m \eqsim$	0.5	1.0	1.5	2.0

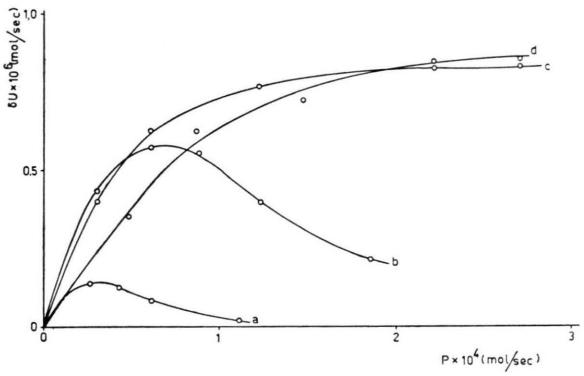

Fig. 12. The variation of the separative power of Column II with the size of the product stream for various m values. Separated mixture: Ne^{20}, Ne^{22}. Working liquid: H_2O. $p=760$ mm Hg. $u=8.4\cdot10^{-6}$ mol/cm² sec.

Curve	a	b	c	d
$m \eqsim$	0.5	1.0	1.5	2.0

The optimum product streams should furthermore vary proportionally to $(1+m^2)^5$, which is also satisfactorily verified by the results in Fig. 12.

A similar set of curves were drawn from the experimental results obtained for the separation of H_2 and D_2 with water as working liquid, which are given in Figs. 14, 15 and 16. Although these curves display more or less the same trend as those for the Ne isotopes, the column efficiencies are markably less than the theoretical values. It is also noticed that if the m value is increased the maximum separative power increases to a certain maximum value after which a decrease ensues. This anomalous phe-

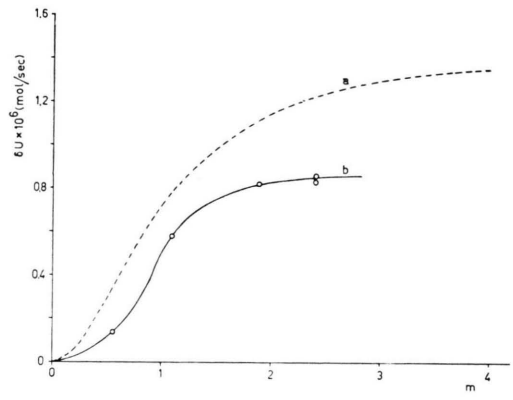

Fig. 13. The effect of the countercurrent flow rate on the maximum separative power. Separated mixture: Ne^{20}, Ne^{22}. Working liquid: H_2O. a: calculated curve. b: experimental curve obtained from the results in Fig. 11.

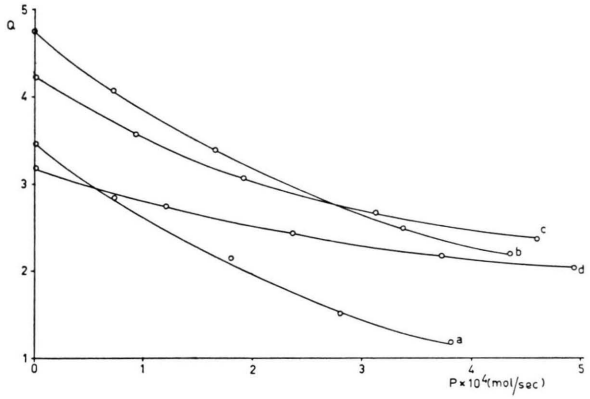

Fig. 14. The effect of the size of the product stream on the separation factor of Column II for various m values. Separated mixture: H_2, D_2. Working liquid: H_2O. $u=8.4\cdot10^{-6}$ mol/cm² sec.

Curve	a	b	c	d
$m \eqsim$	0.5	1.0	1.5	2.0

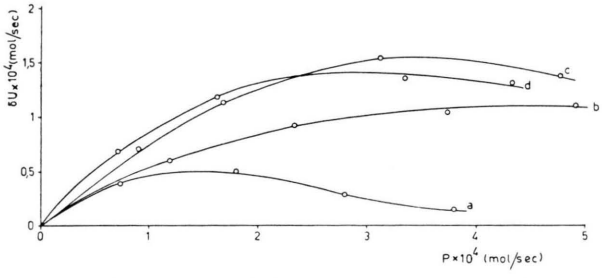

Fig. 15. The variation of the separative power of Column II with the size of the product stream for various m values. Separated mixture: Ne^{20}, Ne^{22}. Working liquid: H_2O. $u=8.4\cdot10^{-6}$ mol/cm² sec.

Curve	a	b	c	d
$m \eqsim$	0.5	1.0	1.5	2.0

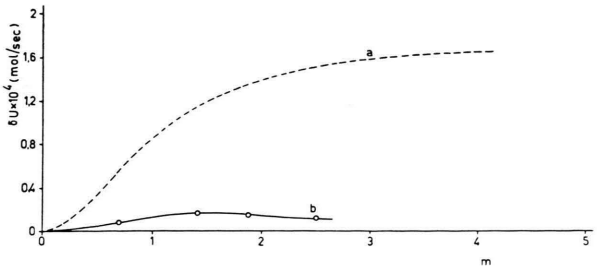

Fig. 16. The effect of the countercurrent flow rate on the maximum separative power. Separated mixture: H_2, D_2. Working liquid: H_2O. a: calculated curve. b: experimental curve obtatined from the results in Fig. 15.

nomenon also appears to be a result of considerable column inefficiency at the relatively excessive countercurrent flow rates. For the efficiencies obtained in these experiments mass diffusion is hardly more economic than the distillation and electrolytical techniques currently used for enriching deuterium. Experiments with a sweep diffusion column are presently conducted in which the separation of H_2 and D_2 is further investigated.

7. Conclusions

According to our results, we are not convinced that the special type of vapour supply tube proposed by GVERDTSITELI et al.[3] is superior to the type of tube used in Column II. The porous type of tubes used by CICHELLI et al.[6] are possibly still the best in that auxiliary vapour emerges homogeneously over the whole exterior surface of the tube. The diffusion resistances of such tubes are presumably also considerable.

Although this study was not intended to elucidate all economic and efficiency aspects of mass diffusion columns it may be concluded from the theoretical treatment and our experimental results that working liquids having high molecular weight (and low heats of evaporation) are superior to more lighter liquids. These liquids ensure large ε values and favourably low optimum countercurrent flow rates. If the gas solubilities of the isotopes are appreciable and the optimum countercurrent flow rates too small, however, columns should be operated at low column pressures. If this is not practically convenient it could be advantageous under certain condition to reside to lighter working liquids. This means, however, that liquids like water have to be used for which the ε values of the most light isotopic gases are small and that much higher countercurrent flow rates will be required, which may cause quite unsatisfactory separation efficiencies.

Acknowledgements

This work is part of the scientific program of the Stichting voor Fundamenteel Onderzoek der Materie (Foundation F.O.M.), supported by the Organisatie voor Zuiver Wetenschappelijk Onderzoek (Z.W.O.) in The Hague. One of us (W. J. DE WET) is employed by the South-African Atomic Energy Board and hereby wishes to acknowledge his gratitude to the Board for monetary support and permission to work at F.O.M.-Laboratory in Amsterdam. He is furthermore indebted to Prof. Dr. J. KISTEMAKER for his hospitality and helpful criticism. — We are thanking Dr. I. E. BOCK and Ir. C. J. G. SLIEKER for many helpful discussions in the early stages of this investigation.

[6] M. T. CICHELLI, W. D. WEATHERFORD, and J. R. BOWMAN, Chem. Eng. Progr. **47**, 123 [1951].